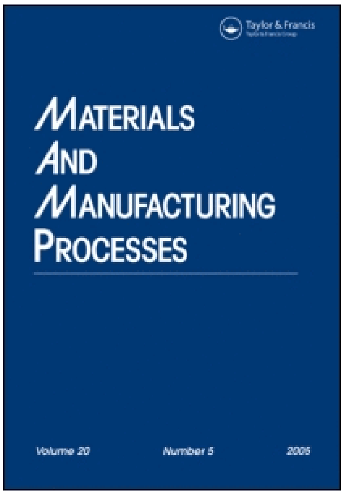

Materials and Manufacturing Processes

Publication details, including instructions for authors and subscription information:
http://www.informaworld.com/smpp/title~content=t713597284

FEM and ANN Analysis in Fine-Blanking Process

F. Djavanroodi[a]; A. Pirgholi[a]; E. Derakhshani[a]
[a] Department of Mechanical Engineering, Iran University of Science and Technology, Tehran, Iran

Online publication date: 02 September 2010

To cite this Article Djavanroodi, F. , Pirgholi, A. and Derakhshani, E.(2010) 'FEM and ANN Analysis in Fine-Blanking Process', Materials and Manufacturing Processes, 25: 8, 864 — 872

To link to this Article: DOI: 10.1080/10426910903367444

URL: http://dx.doi.org/10.1080/10426910903367444

Materials and Manufacturing Processes, 25: 864–872, 2010

ISSN: 1042-6914 print/1532-2475 online
DOI: 10.1080/10426910903367444

FEM and ANN Analysis in Fine-Blanking Process

F. Djavanroodi, A. Pirgholi, and E. Derakhshani

Department of Mechanical Engineering, Iran University of Science and Technology, Tehran, Iran

Fine-blanking (FB) is an effective and economical shearing process that offers a precise and clean cutting-edge finish, eliminates unnecessary secondary operations, and increases quality. In the traditional blanking product development paradigm, the design of the formed product and tooling is usually based on know-how and experience, which are generally obtained through long years of apprenticeship and skilled craftsmanship.

In this study, the possibility of using finite element method (FEM) together with artificial neural networks (ANN) was investigated to analysis the fine-blanking process. Finite element analysis was used to simulate the process with an isotropic elastic–plastic material model. The results compare well with experimental results available in the literature; after confirming the validity of the model with experimental data, a number of parameters such as V-ring height effect, punch and holder force on die-roll, hydrostatic pressure status as an important factor in increasing burnish zone, and accuracy of part and radial stress status as a factor in increasing die erosion, which were also used for training the ANN, were considered. Finally, numerical data were used to train neural networks. The Levenberg–Marquardt (LM) algorithm with three neurons in the hidden layer (LM-3) appeared to be the most optimal topology and gives the best results. It was found that the coefficient of multiple determinations (R^2 value) between the FEM and ANN predicted data is equal to about 0.999 for the size of die-roll, therefore indicating the possibility of FEM and ANN as a powerful design tool for the fine-blanking process.

Keywords Artificial neural networks; Clearance; Die-edge radius; Fine-blanking; Finite element method; Hydrostatic pressure; V-ring.

Introduction

Fine-Blanking Process

Fine-blanking (FB) is generally well known as an effective and economical shearing process that offers a precise and clean cutting-edge finish, eliminates unnecessary secondary operations, and increases quality. This process utilizes triple-action tools: a punch, a stripper with an indented V-ring, and a counterpunch (ejector) to generate a high compressive stress state. Figure 1 shows a comparison between fine-blanking and conventional processes. Nowadays, this technology is being used in automotive, aerospace, and many other industries.

However, in recent years, technical requirements for fine-blanking are more demanding. It is difficult to determine the optimal die design and working parameters by traditional approaches, such as the use of a database or trial-and-error approach. Although, due to large strain concentrated on the blanked zone and crack formation, it is difficult to run an accurate finite element (FE) calculation, the finite element method (FEM) has been verified for fine-blanking [1–4].

In this article, firstly an axisymmetric elastic–plastic, nonlinear analysis was performed by FEM and the effect of clearance on the size of die-roll and punch force was compared with open literature laboratory result [4]. Secondly, after confirming the validity of the model with experimental data, a number of parameters that were subsequently used for training of the artificial neural network (ANN) were also considered. In this study, FEM was used as a tool to clarify the effects of V-ring height, punch, and holder force on die-roll and hydrostatic pressure status as an important factor in increasing burnish zone and accuracy of part and radial stress status as a factor in increasing die erosion.

Artificial Neural Networks

The ANN is a computational network that attempts to simulate the process that occurs in the human brain and nervous system during pattern recognition, information filtering, and functional control [5]. It uses an inductive approach to generalize the input–output relationship to approximate the desired function; such specific capacity is helpful when the case is difficult to derive a mathematical model. Due to this property, its promising applications in product design and development in metal-forming product development as a relationship of performance and behavior of the designed forming system with its design parameters is very difficult to be represented as an explicit mathematical model [6]. There is very little literature work on the use of ANNs in FB. Chan et al. [6] developed an integrated methodology based on FEM simulation of an ANN to approximate the function of design parameters and the performance of designs in such a way that the optimal design can be identified. Fuh et al. [7] used an ANN in estimation of plastic injection molding production cost. Nineteen cost-related factors were considered and historical cost data were use to train the ANN. They reported that the estimation could be more accurate by using different ANN structures for different cost ranges. Raj et al. [8] used FEM and ANN to model the hot upsetting, hot extrusion, and metal cutting processes. The process load was estimated by presenting the required process parameters to the ANN. They showed that it is possible to use an ANN in the

Received July 8, 2009; Accepted August 8, 2009
Address correspondence to Dr. F. Djavanroodi, Ph.D., Department of Mechanical Engineering, Iran University of Science and Technology, Narmak, Tehran 16846-13114, Iran; E-mail: f.roodi@ic.ac.uk

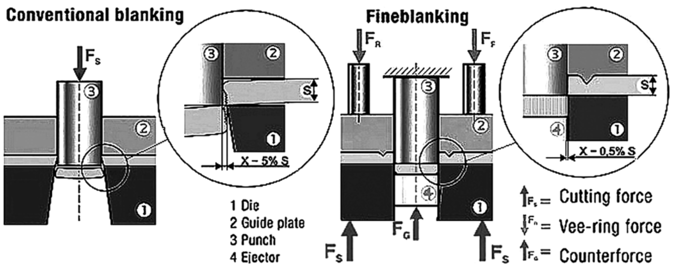

FIGURE 1.—Schematic illustration of one setup for fine-blanking and conventional processes.

automatic selection of tools and real-time monitoring of tool wear. Di Lorenzo et al. [9] applied an ANN to predict ductile fracture in cold-forming operations. They used FEM to predict effective strain, tangential stress, effective stress, maximum principle stress, and mean stress at the critical regions of the workpiece in five forming steps, and those variables were then input to the ANN for estimating the occurrence of ductile fracture. Ko et al. [10] utilized an ANN to evaluate the design in multistage metal-forming to avoid ductile fracture. In their study, a bolts cold-heading process was optimized to demonstrate and validate their proposed design method. Furthermore, Kim et al. [11] utilized the ANN's function approximation ability to find the optimum design to eliminate the underfilling defect of the rib-web product and enhance the dimensional accuracy of the cylindrical pulley. Viswanathan et al. [12] investigated springback of a steel channel-forming process using an ANN and a stepped binder force trajectory. They concluded that the neural network control algorithm is able to effectively capture the nonlinear relationship and interactions of the process parameters. Petterson et al. [13] applied flexible neural networks using a multi-objective predator–prey genetic algorithm to steel plate processing. In their study, data for yield strength and ultimate tensile strength of the rolled slabs in terms of a total of 108 process variables were used. They concluded that nitrogen content of the steel is the most significant input variable. Ciurana et al. [14] studied surface finishing, and geometrical and dimensional features of the grooves/cavities were investigated in a laser micromachining (laser milling) process of hardened AISI H13 tool steel using a pulsed Nd:YAG laser. They successfully developed multiple linear regression and neural network models to predict surface roughness and geometrical and dimensional features. Forsik and Bhadeshia [15] designed and experimentally verified a neural network to model the elongation of neutron-irradiated. Modeling uncertainties due to the lack of experimental data were reported when the model was extrapolated. Ryu and Bhadeshia [16] analyzed a large database on hot-rolled steels and developed a neural network model that estimates the strength as a function of chemical composition and process variables. Wen et al. [17] designed and trained a general regression neural network (GRNN) and a sequential quadratic programming (SQP) method to determine an optimal parameter setting for a die-casting process. They showed that, by combining a GRNN with the SQP algorithm, the trial-and-error process can be eliminated and the model can be used to predict the wear mass losses of the die-casting process.

Analytical analysis of fine-blanking is a very complex process, mainly because of the limited experimental data and analytical functions required for calculations, which usually involves the solution of complex differential equations. In order to simplify this complex process, attempts have been made to combine the ANN and FEM simulation to support the FB process. Figure 2 presents the framework of the methodology used.

FINE-BLANKING MODELING

Simulation with FEM

An example of the FEM simulation model used in this study is shown in Fig. 3: the V-ring indenters formed on both the blank holder and die. The blanked material was AISI 1045 with a thickness of 4.5 mm. The mechanical properties of AISI 1045 were an ultimate tensile strength of

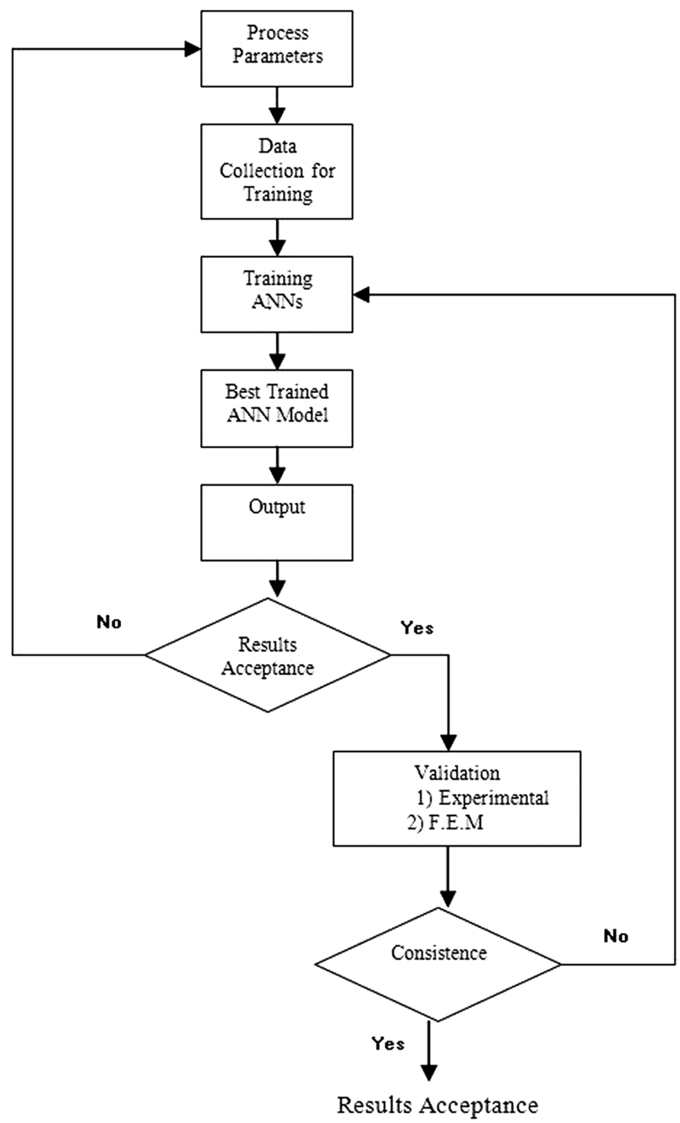

FIGURE 2.—Framework of the methodology used.

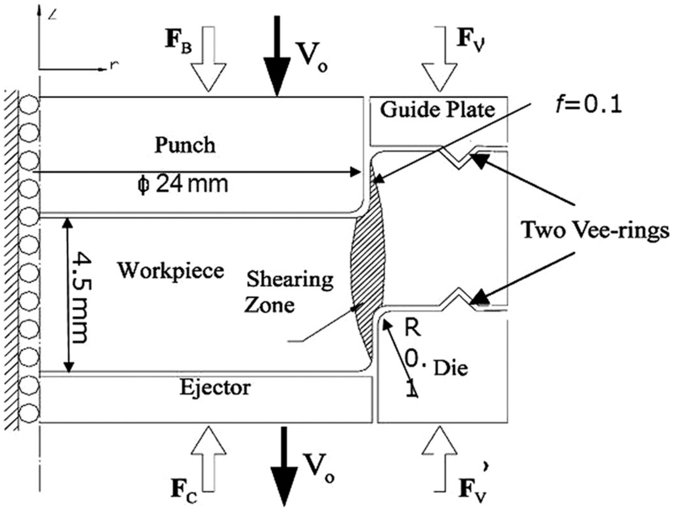

FIGURE 3.—V-ring indenters formed on both the blank holder and die.

585 MPa and an elongation of 12%, as shown in Table 1, and a two-dimensional axisymmetric elastic–plastic, nonlinear analysis was performed by FEM. The mechanical properties and parameters used in FE analysis are shown in Table 1 [4].

Due to the shear band developed during the cutting process in the clearance zone, extra attention was given to the clearance zone. Therefore, a highly fine mesh was generated in the clearance zone. In other areas, mesh sizes are larger to decrease the analysis time. Mesh sensitivity was performed and it was found that at 0.04 mm element size, a stable state of hydrostatic stress was achieved.

Formulation with ANNs

For training of the ANNs the numerical results used were obtained from the FEM after confirming the validation of the model with laboratory results [4]. The back-propagation learning algorithm is used in a feed-forward, single hidden layer network. In the majority of neural networks no transfer functions for the input layer are considered, so neurons in the input layer have no transfer function [18]. A tangent sigmoid (Tansig) transfer function is used as the activation function for the hidden layer. The transfer function used is presented in Eq. (1). The values of the training and test data were normalized to a range of $(-1, 1)$.

$$\mathrm{Tangsig}(z) = 2(1 + \exp(-2z)) - 1 \tag{1}$$

TABLE 1.—FEM simulation conditions.

Simulation model	Axisymmetric model
Workpiece	Elasto-plastic
Punch/die	Rigid
Blank holder	Rigid
Counterpunch	Rigid
Blanked material	S45C ($\sigma_B = 585\,\mathrm{MPa}$, $\lambda = 12\%$) $\bar{\sigma} = k\bar{\varepsilon}^n$ ($n = 0.11$, $k = 1020$)
Friction coefficient (μ)	0.1

where z is the weighted sum of the input. A computer program has been performed for the ANN simulation and the data pattern from the FEM were used for training of the network. Five numbers of available data were randomly selected and used as test data set. Statistical methods, including mean square error (MSE), root-mean-squared (RMS), absolute fraction of variance (R^2), and coefficient of variation in percentage (cov) values, were used for comparison. Error during the learning is RMS and is defined as follows:

$$RMS = \left(1/p \sum_j |t_j - o_j|^2\right)^{1/2} \tag{2}$$

In addition, R^2 and coefficient of variation in percentage (cov) are defined as follows, respectively:

$$R^2 = 1 - \left(\frac{\sum_j (t_j - o_j)^2}{\sum_j (o_j)^2}\right) \tag{3}$$

$$\mathrm{cov} = \frac{RMS}{o_{\mathrm{mean}}} \times 100 \tag{4}$$

where t is target value, o is output value, p is pattern, and o_{mean} is the mean value of all output data [19].

The performance of the network can be evaluated by the mean square error (MSE), which is defined as:

$$MSE = 1/p \sum_j |t_j - o_j|^2 \tag{5}$$

Inputs and outputs are normalized in the $(-1, 1)$ range as shown in Eq. (6).

$$v_n = 2(v_R - v_{\mathrm{Min}})/(v_{\mathrm{Max}} - v_{\mathrm{Min}}) - 1 \tag{6}$$

Variants of the algorithm used in the study are scaled conjugate gradient (SCG), Pola–Ribiere conjugate gradient (CGP), and Levenberg–Marquardt (LM). The decrease of the mean square error (MSE) during the training process is shown in Fig. 4. The coefficient of multiple determination (R^2 value) obtained is 0.999 for the LM algorithm, which is satisfactory (Fig. 4).

RESULTS AND DISCUSSION

Results of FEM

Figure 5 shows the effect of clearance on width (a) and depth (b) of the die-roll. With increasing clearance, the width and depth of the die-roll increase, which is in good agreement with experimental work performed in Kwak et al. [4]. The dependence of clearance on die-roll size is shown in Fig. 6. As can be seen, with decreasing clearance, distribution of equivalent stress and strain becomes thinner and a smaller area in the clearance zone is deformed. Thus, with a small clearance, the size of the die-roll and deformation zone become smaller and it is able to produce more precision parts.

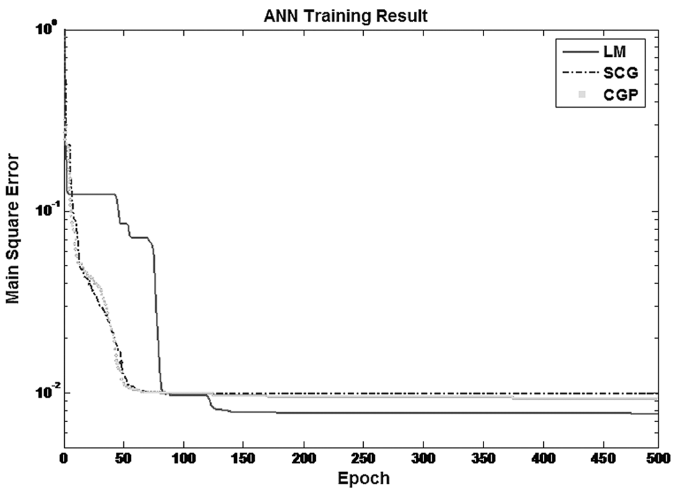

FIGURE 4.—Training results based on the 3-3-2 configuration.

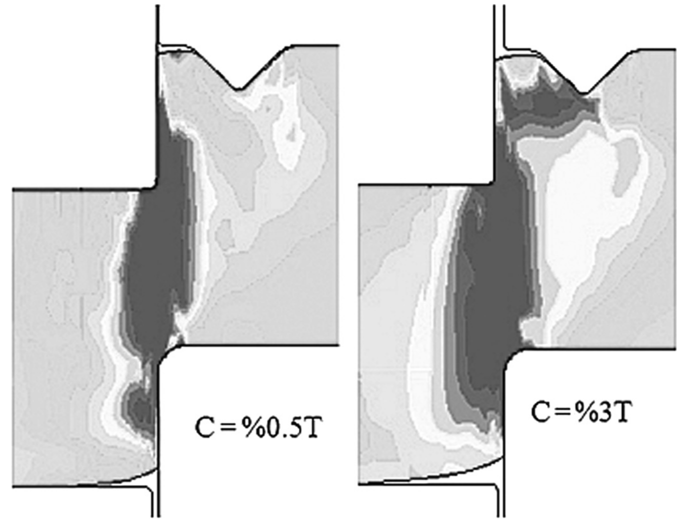

FIGURE 6.—Die-roll size and distribution of stress depend on clearance.

Figure 7 shows that with decreasing clearance, the maximum of punch force increases slightly. These results are consistent with engineering insight and have a good accordance with the experiment results [4]. Punch penetration in this analysis was taken to be 50% of sheet thickness.

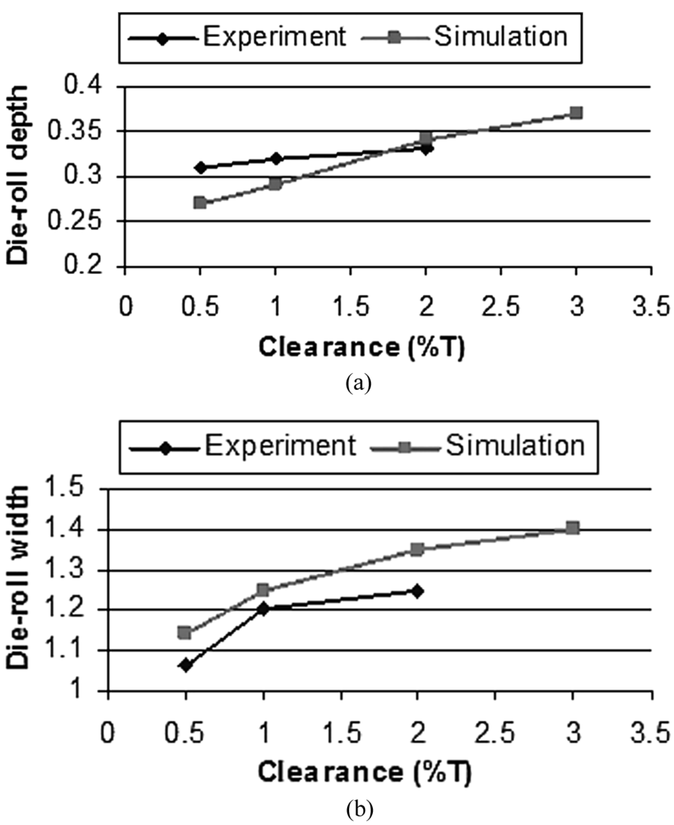

FIGURE 5.—Variation of die-roll size (mm) according to die clearance (percentage of sheet thickness).

The radius of the edge die does not have much effect on the size of the die-roll and accuracy of the product, as shown in Fig. 8. Therefore, it can be used for better extruding of material in the clearance zone.

Figure 9 shows the effect of V-ring height on the state of hydrostatic pressure after V-ring action and before punch movement. With increasing V-ring height, hydrostatic pressure increases and ductile fracture is delayed. Therefore, the burnish zone and accuracy will increase.

In Fig. 10 it is observed that with increasing V-ring height, the size of the die-roll decreases. In accordance with Figs. 9 and 10, utilizing a V-ring in the die and sheet holder increases hydrostatic pressure in the clearance zone, especially on the side of the die. Also, the size of the

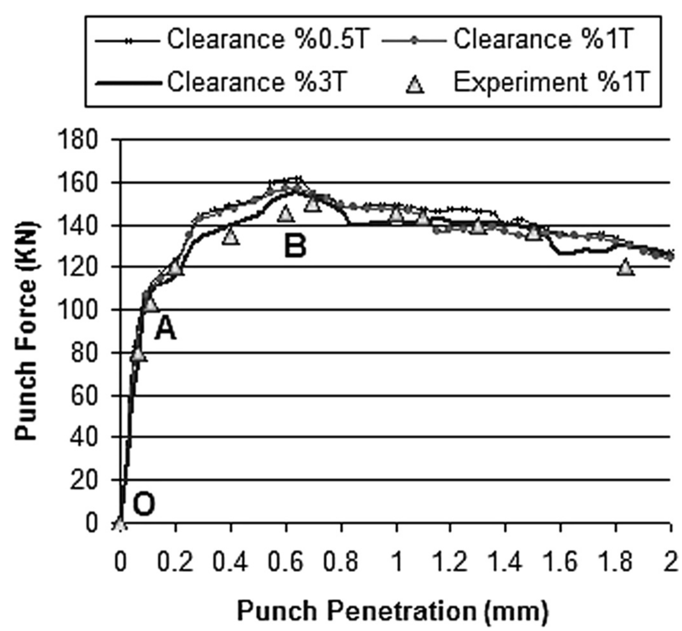

FIGURE 7.—The simulation result of load–stroke curve.

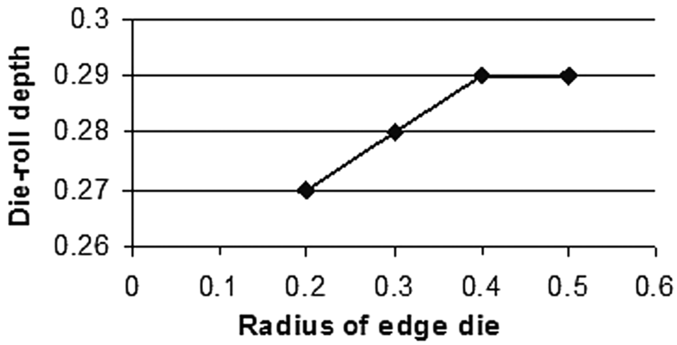

FIGURE 8.—Variation of die-roll depth (mm) according to radius of the edge die (mm).

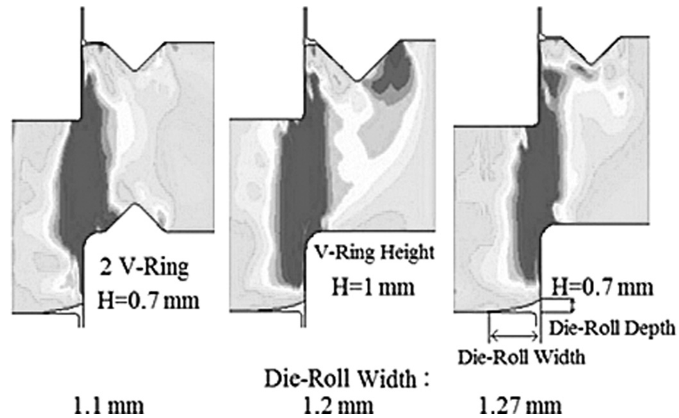

FIGURE 10.—Variation of die-roll size according to V-ring height.

die-roll will decrease. But in accordance with Fig. 11, the inverse radial stress in the thickness direction will increase with increasing V-ring height and decreasing distance from the clearance zone after V-ring action and before punch movement. Therefore, torque and subsequently dishing will increase.

Utilizing a counterpunch will decrease this imperfection. Also, utilizing a V-ring in dies and sheet holder regulates radial stress in the clearance zone.

Figure 12 shows a punch penetrates radial stress increase in sidewall of punch, with increasing V-ring height. This will cause friction and erosion of the tool to increase and a subsequent decrease in tool life.

The effect of counterpunch force and sheet holder (V-ring) on hydrostatic pressure in the clearance zone and radial stress in the sidewall of the punch and die is illustrated in Figs. 13 and 14. With increasing force of the counterpunch and sheet holder, hydrostatic pressure will increase. At the same time, as shown in Fig. 14, radial stress in the sidewall of the punch and die will increase, which will cause erosion of the tool.

Radial stress distribution of the tool sidewall is illustrated in Fig. 15. Increasing forces without a V-ring has little effect on hydrostatic pressure. Also, utilization of a V-ring in both the die and sheet holder (2V-ring) is very effective without increasing force in the counterpunch and sheet holder.

Results of ANNs

The ANN was built and trained in a Matlab™ environment [20]. The training process adjusts the weight of each neuron to an appropriate value. There are many available training algorithms, but the most popular one is the error back-propagation algorithm [5–7] and it was used in this study. There is no strict rule for designing the ANN structure. However, the number of neurons in the hidden layers is critical to determine the complexity level of the function. In order to calculate the depth of the die-roll (D) and width of the die-roll (W), mathematical formulations can be derived from the resulting weights and the activation functions used in the ANN. Because the regression coefficients obtained from both the training and testing of the ANNs were extremely good in both cases, it is believed that the results thus obtained would be accurate. As expected, the best approach, which performed with minimal errors, is the LM algorithm with three neurons [18]. Levenberg–Marquardt (LM) back-propagation training was repeatedly applied until satisfactory training was achieved.

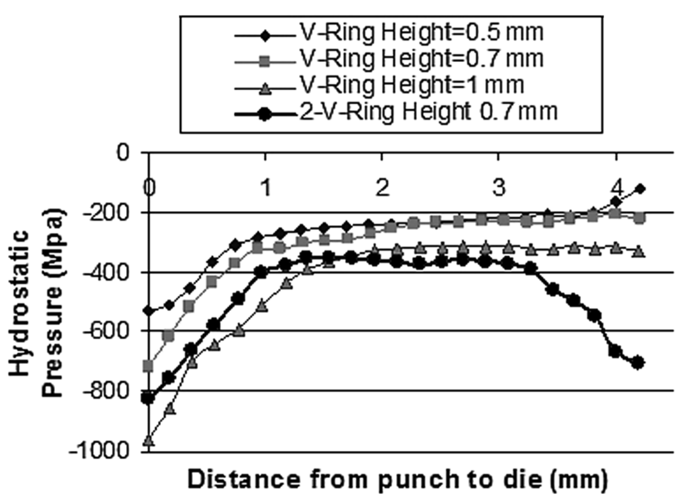

FIGURE 9.—Variation of hydrostatic pressure according to V-ring height.

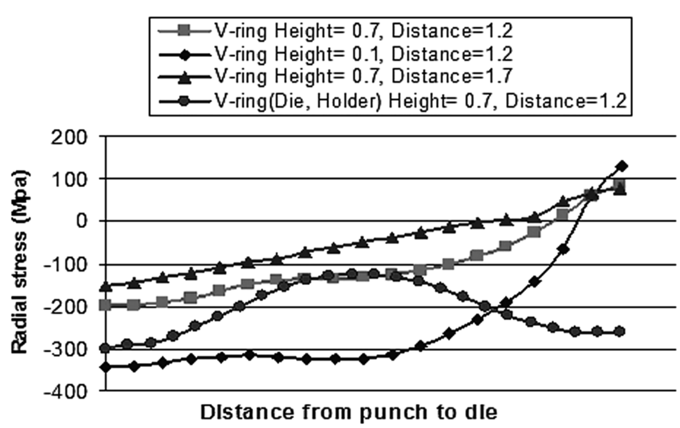

FIGURE 11.—Variation of radial stress in the clearance zone according to V-ring height and distance.

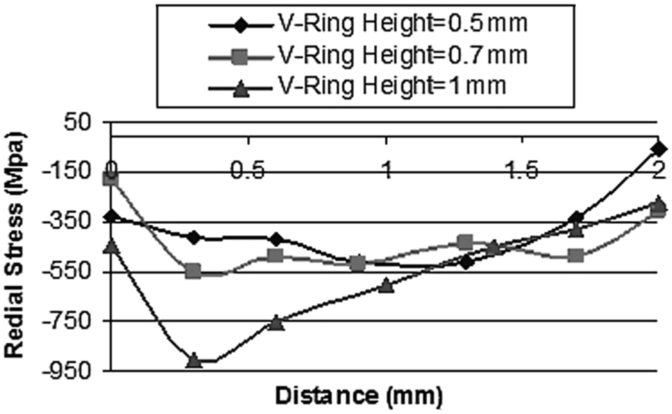

FIGURE 12.—Variation of radial stress in the sidewall of the punch according to V-ring height.

The configuration 3-3-2 appeared to be the most optimal topology for this application. It would have been possible to optimize the topology of the neural network utilizing multi-objective genetic algorithms for training of the neural network. In this method the number of nodes in the hidden layer, the architecture of the network, and the weights can be taken as variables, and a Pareto front can be constructed by minimizing the training error along with the network size [21–25].

Figure 16 shows the architecture of the ANN used for the depth and width of die-roll prediction. The radius of edge die (R), V-ring height (H), and clearance (C) are the input data and the depth of die-roll (D) and width of die-roll (W) are the actual outputs.

From the data presented in Table 2, depth of die-roll (D) and values of the LM algorithm with three neurons in the hidden layer (LM-3) appeared to be the most optimal topology.

The regression curves of the output variable die-roll depth (D) and die-roll width (W) for the test data set are shown in Figs. 17 and 18, respectively. It should be noted that these

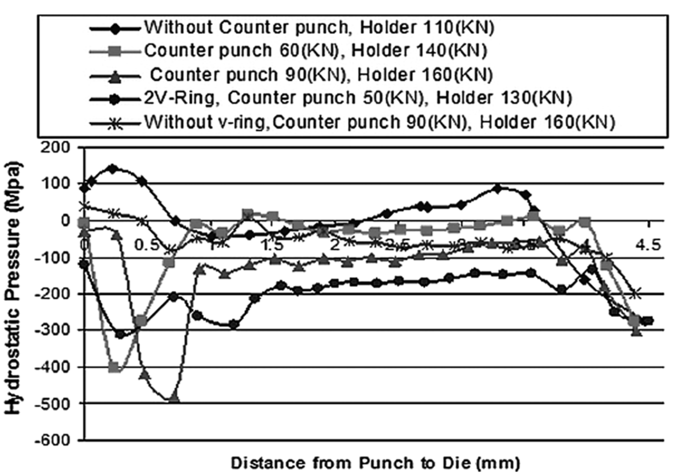

FIGURE 13.—Variation of hydrostatic pressure according to punch and sheet holder force.

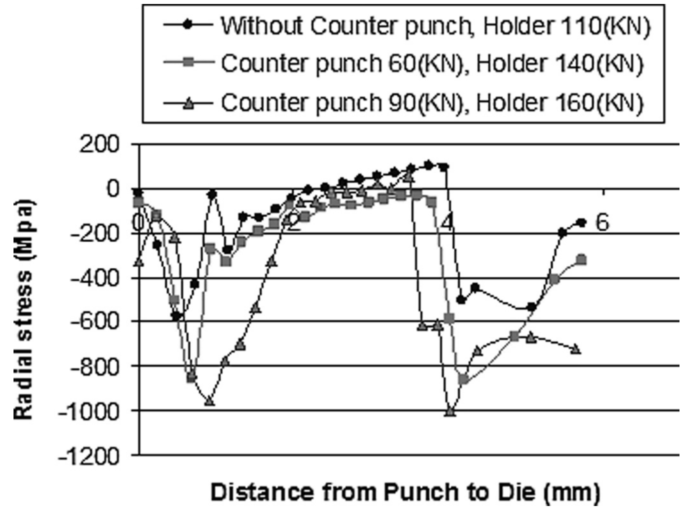

FIGURE 14.—Variation of radial stress in the clearance zone according to punch and sheet holder force.

FIGURE 15.—Distribution of radial stress in the sidewall of the tool.

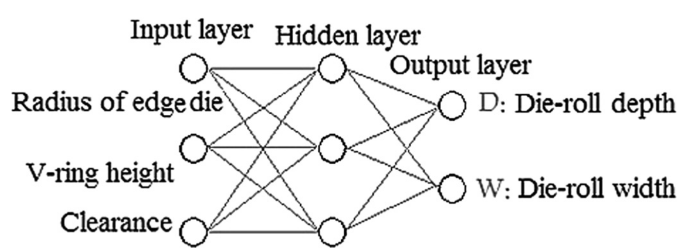

FIGURE 16.—ANN structure used for C_d formulation prediction.

TABLE 2.—Statistical values of the training process for depth of the die.

Neurons	MSE	RMS	R^2	Cov
3	0.0003	0.0185	0.9998	1.4214
4	0.0004	0.0203	0.9998	1.5675
5	0.0465	0.2157	0.9777	15.2537
6	0.0007	0.027	0.9996	2.0896
7	0.0016	0.0395	0.9991	3.0529
8	0.0006	0.0255	0.9996	1.9521
9	0.0061	0.0781	0.9964	6.0751
10	0.0033	0.0575	0.9981	4.3717

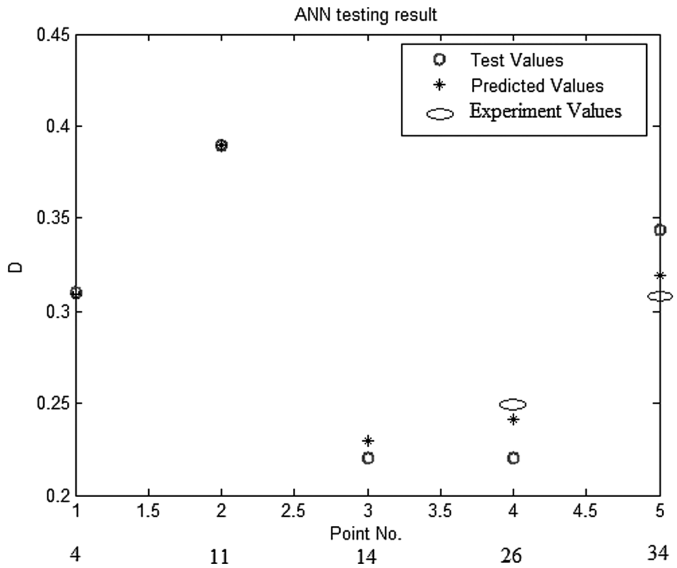

FIGURE 17.—Comparison of actual and ANN-predicted values for D (test data set).

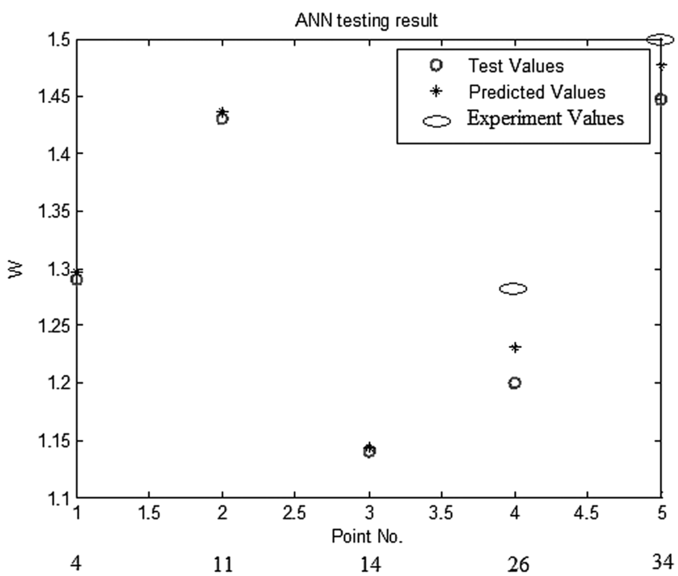

FIGURE 18.—Comparison of actual and ANN-predicted values for W (test data set).

TABLE 3.—Statistical values of test process for depth of the die.

No.	D: NN	D: FEM	D: EXP	% Error (ANN and EXP)
4	0.31	0.31		
11	0.39	0.39		
14	0.23	0.22		
26	0.24	0.22	0.25	4.00
34	0.32	0.34	0.31	4.00

TABLE 4.—Statistical values of test process for width of the die.

No.	W: NN	W: FEM	W: EXP	% Error (ANN and EXP)
4	1.3	1.29		
11	1.44	1.43		
14	1.15	1.14		
26	1.23	1.2	1.31	6.1
34	1.47	1.45	1.5	2.00

TABLE 5.—Statistical values of the test process for width of the die.

Neurons	MSE	RMS	R^2	Cov
3	0.0002	0.0138	0.9982	4.3664
4	0.0002	0.014	0.9981	4.493
5	0.0093	0.0967	0.9398	26.3061
6	0.0015	0.0389	0.984	13.1032
7	0.0002	0.0154	0.9977	5.0081
8	0.0006	0.0246	0.9943	7.7505
9	0.0015	0.0387	0.9857	12.4123
10	0.0032	0.0569	0.9704	18.9873

TABLE 6.—Weight values obtained using LM algorithm with three neurons for the input layer.

	$Ei = C1i * R + C2i * V + C3i * C + C4i$			
i	$C1i$	$C2i$	$C3i$	$C4i$
1	−6.9647	25.0233	34.2698	−12.0929
2	1.4715	−4.2241	18.6206	−1.9756
3	0.0561	−0.2675	0.4009	0.1767

TABLE 7.—Weight values obtained using LM algorithm with three neurons for the hidden layer.

	$\text{Out}(i) = B1i * F_1 + B2i * F_2 + B3i * F_3 + B4i$			
i	$B1i$	$B2i$	$B3i$	$B4i$
1	−0.1053	−0.1148	1.8536	−0.3334
2	−0.1270	−0.0609	1.6224	−0.3286

data were completely unknown to the network. Tables 3 and 4 show the comparison of the ANN, FEM, and experimental results for the depth and width of the die.

In Table 5, the statistical values of the test process for the width of die are shown. As can be seen, the error is very small. Neurons in the input layer have no transfer function. A tangent sigmoid transfer function has been used.

$$f(E_i) = 2/(1 + \exp(-2 \times E_i)) - 1 \tag{7}$$

where E_i is the weighted sum of the input and should be taken from Table 6. Finally, the outputs of the ANN obtain are shown in Table 7.

Conclusion

1. Even with the FEM simulation technology, it is impossible to conduct all simulations for any given point in the process. Fine-blanking usually involves many process parameters. A subtle change of any parameter will constitute a new scenario and a new simulation is needed to explore its behaviors and performance. It is not pragmatic to find the optimal solution through one-by-one simulation. To address this issue, a new approach was used, a combination of FEM and ANN. This combination helps to reduce the simulation time and make it possible to search for the optimal process parameters in fine-blanking. All the validation results show that the estimation of ANN can achieve a satisfactory level.
2. As a result of the FEM study, the following conclusions can be realized: With decreasing clearance and increasing V-ring height, hydrostatic pressure increases and die-roll size decreases. Also, with increasing force of the counterpunch and sheet holder, hydrostatic pressure increases; therefore, quality and accuracy of the product will increase. However, with these qualifications, radial stress increases in the sidewall of the tool, and subsequently friction and erosion of the tool increase. This will cause the life of tool and press to decrease. Utilizing a V-ring in both the die and sheet holder is more effective for quality and accuracy of the product. Therefore, we can use minor force of the tool and subsequently the life of the tool and press increase. In the other words, utilizing a V-ring in both the die and sheet holder is more economical in fine-blanking processes.

Nomenclature

CGP	Pola-Ribiere conjugate gradient
cov	Coefficient of variation (%)
LM	Levenberg–Marquardt
MSE	Mean square error
o_{mean}	Mean value of all output data
R^2	Absolute fraction of variance (R^2)
RMS	Root-mean-squared
SCG	Scaled conjugate gradient
$v_{\max}$	Maximum value in all the values for related variables
$v_{\min}$	Minimum value in all the values for related variables
v_N	Value to be normalized
v_R	Value will be normalized
z	Weighted sum of the inputs

Subscripts

o	Output value
p	Pattern
t	Target value

References

1. Thipprakmas, S.; Jin, M.; Murakawa, M. An investigation of material flow analysis in fine-blanking process. Journal of Materials Processing Technology **2007**, *192–193*, 237–242.
2. Thipprakmas, S.; Jin, M.; Tomokazu, K.; Katsuhiro, Y.; Murakawa, M. Prediction of fine-blanked surface characteristics using the finite element method (FEM). Journal of Materials Processing Technology **2008**, *198*, 391–398.
3. Thipprakmas, S. Finite-element analysis of V-ring indenter mechanism in fine-blanking process. Materials & Design **2009**, *30*(3), 526–531.
4. Kwak, T.S.; Kim, Y.J.; Bae, W.B. Finite element analysis on the effect of die clearance on shear planes in fine-blanking. Journal of Materials Processing Technology **2002**, *130–131*, 462–468.
5. Hagan, M.T.; Demuth, H.B.; Beale, M. *Neural Network Design*; PWS Publishing: Boston, MA, 1996.
6. Chan, W.L.; Fu, M.W.; Lu, J. An integrated FEM and ANN methodology for metal-formed product design. Engineering Application of Artificial Intelligence **2008**, *21*, 1170–1181.
7. Fu, M.W.; Yong, M.S.; Tong, K.K.; Muramatsu, T. A methodology for evaluation of metal forming system design and performance via CAE simulation. International Journal of Production Research **2006**, *44*, 1075–1092.
8. Raj, K.H; Sharma, R.S.; Srivastava, S.; Patvardhan, C. Modeling of manufacturing processes with ANNs for intelligent manufacturing. International Journal of Machine Tools and Manufacture **2000**, *40*, 851–868.
9. Di Lorenzo, R.; Ingarao, G.; Micari, F. On the use of artificial intelligence tools for fracture forecast in cold forming operations. Journal of Materials Processing Technology **2006**, *177*, 315–318.
10. Ko, D.C.; Kim, D.H.; Kim, B.M.; Choi, J.C. Methodology of perform design considering workability in metal forming by the artificial neural network and Taguchi method. Journal of Materials Processing Technology **1998**, *80–81*, 487–492.
11. Kim, D.J.; Kim, B.M. Application of neural network and FEM for metal forming processes. International Journal of Machine Tools and Manufacture **2000**, *40*, 911–925.
12. Viswanathan, V.; Kinsey, B.; Cao, J. Experimental implementation of neural network springback control for sheet metal forming. Journal of Materials and Technology **2003**, *124*, 141–147.
13. Pettersson, F.; Chakraborti, N.; Singh, S.B. Neural networks analysis of steel plate processing augmented by multi-objective genetic algorithms. Steel Research International **2007**, *78* (12), 890–898.
14. Ciurana, J.; Arias, G.; Ozel, T. Neural network modeling and particle swarm optimization (PSO) of process parameters in pulsed laser micromachining of hardened AISI H13 steel. Materials and Manufacturing Processes **2009**, *24*, 358–368.
15. Forsik, S.; Bhadeshia, H.K.D.H. Elongation of irradiated steels. Materials and Manufacturing Processes **2009**, *24*, 130–137.
16. Ryu, J.H.; Bhadeshia, H.K.D.H. Contribution of microalloying to the strength of hot-rolled steels. Materials and Manufacturing Processes **2009**, *24*, 138–144.

17. Wen, J.L.; Shie, J.R.; Yang, Y.K. Optimization of a wear property of die cast AZ91D components via a neural network. Materials and Manufacturing Processes **2009**, *24*, 400–408.
18. Haykin, S. *Neural Networks: A Comprehensive Foundation*; Prentice Hall: Englewood Cliffs, NJ, 1999.
19. Bechtler, H.; Browne, M.W.; Bansal, P.K.; Kecman, V. New approach to dynamic modeling of vapour-compression liquid chillers. Artificial neural networks. Applied Thermal Engineering **2001**, *21*, 941–953.
20. MATLAB Software, Version 5, 2008.
21. Pettersson, F.; Chakraborti, N.; Saxen, H. A genetic algorithms based multi-objective neural net applied to noisy blast furnace data. Applied Soft Computing **2007**, *7*, 387–397.
22. Mikko, H.; Pettersson, F.; Chakraborti, N.; Saxen, H. Modeling noisy blast furnace data using gentic algorithms and nural networks. Steel Research International **2006**, *77* (2), 75–81.
23. Pettersson, F.; Biswas, A.; Sen, P.K.; Saxén, H.; Chakraborti, N. Analyzing leaching data for low-grade manganese ore using neural nets and multiobjective genetic algorithms. Materials and Manufacturing Processes **2009**, *24*, 320–330.
24. Pettersson, F.; Suh, C.; Saxén, H.; Rajan, K.; Chakraborti, N. Analyzing sparse data for nitride spinels using data mining, neural networks, and multiobjective genetic algorithms. Materials and Manufacturing Processes **2009**, *24*, 2–9.
25. Bhattacharya, B.; Kumar, G.R.D.; Agarwal, A.; Erkoç, S.; Singh, A.; Chakraborti, N. Analyzing Fe–Zn system using molecular dynamics, evolutionary neural nets and multi-objective genetic algorithms. Computational Materials Science **2009**, *46*, 821-827.